Spin-dependent electronic states and magnetoconductance in a magnetic quantum antidot

2000 J. Phys.: Condens. Matter 12 3359

(http://iopscience.iop.org/0953-8984/12/14/312)

J. Phys.: Condens. Matter **12** (2000) 3359–3367. Printed in the UK PII: S0953-8984(00)07278-7

Spin-dependent electronic states and magnetoconductance in a magnetic quantum antidot

Yong Guo†‡, Bin Wang†, Hui Hu†, Jing-Zhi Yu‡, Bing-Lin Gu† and Yoshiyuki Kawazoe‡

† Department of Physics, Tsinghua University, Beijing 100084, People's Republic of China
‡ Institute for Materials Research, Tohoku University, Sendai 980-8577, Japan

Received 27 August 1999, in final form 17 February 2000

Abstract. We investigate the electron spin effect on quantum states and magnetoconductance in a magnetic quantum antidot with inhomogeneous distribution of the magnetic field. It is shown that the interaction of the electron spin with the inhomogeneous magnetic field results in further splitting of the energy levels. The predicted value of the splitting is closely related to the angular momentum quantum number and the parameters of the magnetic quantum antidot. Spin-dependent magnetoconductance is very different from that in the case where the spin effect is not included. More and shallower dips appear in the spin-dependent magnetoconductance spectra.

1. Introduction

Recently the interaction of two-dimensional electron gas (2DEG) with an inhomogeneous perpendicular magnetic field has attracted much attention both theoretically and experimentally [1–20]. It has become possible to fabricate 'magnetic dots' with diameter 10 to 30 nm and height 30 to 100 nm by using the scanning tunnelling microscope lithographic technique [1, 3]. A magnetic antidot has a magnetic field profile with a simple disk geometry where the field is zero inside and non-zero and uniform outside the antidot, i.e., $B(r) = B_0\theta(r - r_0)$, where r_0 is the radius of the antidot with the origin at the geometrical centre of the cross junction. One can think of the magnetic antidot profile as resulting from placing a superconducting disk or cylinder on top of the cross junction [14], which, due to the Meissner effect, screens the region immediately below it from the externally applied magnetic field. The magnetic antidot is fundamentally different from the usual quantum dot as:

(1) the electrons are confined magnetically;
(2) the confinement potential is inherently non-parabolic; and
(3) the dot contains a finite number of electrons where the filling of the dot is a discrete function of the strength of the confinement (magnetic field).

Theoretically, quantum states and transport properties in the magnetic antidot have been discussed by several research groups. Among them, Peeters, Matulis, and Ibrahim [16] presented the energy levels in the magnetic antidot, while Reijniers, Peeters, and Matulis [17] further performed a more detailed and complete study of the bound states of such a system and calculated the absorption spectrum. Solimany and Kramer [18] solved the classical and quantum mechanical equations for a magnetically confined quantum dot and discussed the

0953-8984/00/143359+09$30.00

eigenenergies. Recently, Sim *et al* [19] investigated the formation of magnetic edge states along with the corresponding classical trajectories.

More recently, there has been increased interest in electronic spin polarization in solid-state systems [21], fuelled by the possibility of producing efficient photoemitters with a high degree of polarization of the electron beam, creating spin-memory devices [22] and spin transistors [23] as well as exploiting the properties of spin coherence for quantum computation. The idea of electronic devices that exploit both the charge and spin of an electron for their operation has given rise to the new field of 'spintronics', literally spin electronics [24], in which the direction an electron spin is pointing in is just as important as its charge.

It is clear that electronic states and transport properties in the magnetic quantum antidot depend not only on the structure but also on the direction of the electron spin. However, up to now, the spin effect has been overlooked. In the present paper, we take a step forward and make a more detailed study of the spin-dependent energy spectrum and magnetoconductance in such a magnetically confined system.

2. Theory

The model system that we consider here is composed of an electron moving in the (x, y) plane under the influence of a perpendicular magnetic field in the z-direction, which is non-zero except within a cylinder of radius r_0. Although this is an extreme situation, it contains the essential physics of the problem. The distribution of the magnetic field in cylindrical coordinates is described by

$$\vec{B}(\vec{r}) = \begin{cases} B\hat{z} & (r > r_0) \\ 0 & (r < r_0). \end{cases} \tag{1}$$

The corresponding vector potential in cylindrical coordinates is then given by

$$\vec{A}(\vec{r}) = \begin{cases} \dfrac{(r^2 - r_0^2)B}{2r}\hat{\theta} & (r > r_0) \\ 0 & (r < r_0). \end{cases} \tag{2}$$

Including the electron spin effect, the single-particle Schrödinger equation for a two-dimensional magnetic quantum antidot is as follows [20]:

$$\left[\frac{1}{2m^*}(\vec{P} + e\vec{A})^2 + \frac{eg^*}{2m^*}\frac{\sigma\hbar}{2}B_z\right]\Psi(\vec{r}) = E\Psi(\vec{r}) \tag{3}$$

where m^* is the effective mass of the electron, e the proton charge, $\vec{P}$ the momentum of the electron, g^* the effective Landé g-factor of the electron in a real 2DEG realized using a semiconductor, $\sigma = \pm 1$ the eigenvalues of the Pauli matrix for spin-up/down electrons, and E the electron energy. For GaAs, we have $g^* = 0.44$ [20]; m^* can be taken as $0.067m_e$ (m_e is the free-electron mass). We solve the Schrödinger equation in two parts, outside and inside the dot, respectively. The wave functions and the energies are easily determined from the continuity of the wave functions and their derivatives at the boundary of the dot. Due to the cylindrical symmetry of the problem, the wave function can be written as

$$\Psi_{nms_z}(\vec{r}) = R_{nm}(r)\mathrm{e}^{\mathrm{i}m\theta}\chi(s_z) \tag{4}$$

where m is the angular momentum quantum number, n (=0, 1, 2, ...) is the number of nodes in the radial wave function, and $\chi(s_z)$ is the spin wave function. The equation for the radial part is written as

$$\left(\frac{\mathrm{d}^2}{\mathrm{d}r^2}+\frac{1}{r}\frac{\mathrm{d}}{\mathrm{d}r}-\frac{m^2}{r^2}+2E\right)R_{nm}^{(1)}(r)=0 \qquad (r<r_0) \tag{5}$$

$$\left\{\frac{\mathrm{d}^2}{\mathrm{d}r^2}+\frac{1}{r}\frac{\mathrm{d}}{\mathrm{d}r}-\frac{(m-s)^2}{r^2}-r^2+2[E-(m-s+z)]\right\}R_{nm}^{(2)}(r)=0 \qquad (r\geqslant r_0). \tag{6}$$

Here $R_{nm}^{(1)}$ is expressed as $C_1 J_{|m|}(\sqrt{2E}r)$, where the function J_m is the Bessel function of order m; $R_{nm}^{(2)}(r) = C_2 r^{|m-s|}\mathrm{e}^{-r^2/2}U(a,b;r^2)$, where $U(a,b;r^2)$ is the confluent hypergeometric function; $z = g^*\sigma/2$. In this case, all quantities are expressed in dimensionless units by allowing $\hbar\omega_L$ ($=\hbar eB/(2m^*)$) and the inverse length $\beta = \sqrt{m^*\omega_L/\hbar}$ to be 1. $s = \pi r_0^2 B/\phi_0$ is a scale parameter which represents the number of missing magnetic flux quanta within the dot [19], and ϕ_0 ($=h/e$) the flux quantum. For spin-up electrons, $\sigma = 1$,

$$a = -[E-(m-s)-|m-s|-z-1]/2 \qquad b = |m_{eff}|+1$$

and $m_{eff} = m - s$. For spin-down electrons, $\sigma = -1$ and

$$a = -[E-(m-s)-|m-s|-z-1]/2.$$

Since there is no magnetic field inside the magnetic dot, the magnetic edge states may not enclose the magnetic flux, resulting in missing flux quanta; these are absent in the edge states formed by electrostatic confinements.

For a two-dimensional conductor with a magnetic quantum antidot at the centre, we can calculate the two-terminal magnetoconductance, which is the sum of the Hall conductance and the magnetic-edge-channel-related conductance. In the ν quantum Hall plateau region, the Hall conductance is $G_H = \nu e^2/h$, where ν is the Landau-level filling factor. In analysing the conductance oscillations in their measured transport data for semiconductor quantum dots, Persson *et al* [25] introduced a model with an appealing conceptual simplicity. The principal idea is that leads only represent a small perturbation of an otherwise perfectly circular dot. In practice, the only effect of the leads would be to make the individual energy levels of the dot Lorentzian broadened while the overall level structure would remain essentially intact. This is to be expected for a non-interacting system in the tunnelling regime, i.e., when the Fermi energy is below the first subband threshold and the dot is only weakly coupled to its surroundings. For the case where resonant energy levels are evidently separated, near resonant energy levels, the coefficient of transmission through the structure can be calculated by using the Breit–Wigner formula [26, 27]. Similarly to the conductance in large circular semiconductor quantum dots [26], at zero temperature, the conductance which is related to magnetic edge channels may now be obtained by summation over the Lorentzian-shaped transmission coefficient

$$T_{nm\sigma}(B) = \Gamma_{nm\sigma}^2/\{[E_F - E_{nm\sigma}(B)]^2 + \Gamma_{nm\sigma}^2\}.$$

That is,

$$G_M = -\frac{e^2}{h}\sum_{n,m,\sigma} T_{nm\sigma} \tag{7}$$

where E_F is the Fermi energy, $\Gamma_{nm\sigma}$ the elastic resonance width which is introduced by the effect of the leads, and $E_{nm\sigma}$ the eigenenergy of the electron. Therefore, taking the spin effect into account, the magnetoconductance is expressed as [19]

$$G(B) = \frac{e^2}{h}\left[\nu - \sum_{n,m,\sigma}\frac{\Gamma_{nm\sigma}^2}{[E_F - E_{nm\sigma}(B)]^2 + \Gamma_{nm\sigma}^2}\right]. \tag{8}$$

3. Results and discussion

In this section, we calculate exactly and discuss the single-electron eigenstates and transport properties of a magnetic quantum antidot, for which the spin effect is taken into account. Figure 1 presents the estimated dependence of the energy eigenvalues in the magnetic quantum antidot on the angular momentum m. The solid, dotted, and dash–dotted curves correspond to the case without spin ($\sigma = 0$), the spin-up case ($\sigma = +1$), and the spin-down case ($\sigma = -1$), respectively. To allow comparison with reference [19], in this figure and the following ones, the energy is in units of $\hbar\omega_L$ at $r_0 = 500$ Å and $B = 2.633$ T (corresponding to $s = 5$ in reference [19]). In contrast to the case for a homogeneous magnetic field, the eigenvalues are not degenerate with respect to the angular momentum. The degeneracy of the Landau levels is removed. It can be seen that the lowest energy state occurs at $m = 0$. This result indicates that the inhomogeneity of the magnetic field perturbs mostly the states near the boundary of the quantum dot, and this perturbation is caused by the missing flux quanta s. The energy levels increase slowly with the decrease of the angular momentum m for $m < 0$, while they increase rapidly with the incrementing of m for $m > 0$. For the 2DEG in a uniform magnetic field, the eigenstates are described by the degenerate Landau levels, $E_i = \hbar\omega_c(i + 1/2)$, where $\omega_c = eB/m^*$. In the absence of the magnetic field, for half-integer spins the classical twofold degeneracy remains due to Kramers' degeneracy. However, in the presence of the magnetic field, the degeneracy of the energy levels is lifted and the energy levels split when the spin effect is taken into account. The energy spectra for spin-up and spin-down electrons are considerably different from each other, especially for $m < 0$. The levels are lifted for spin-up electrons, while for spin-down electrons the levels are lowered. However, in an inhomogeneous magnetically confined system, the main discrepancy with respect to the case of the uniform magnetic field is that the splitting features are not only related to the direction of the electron

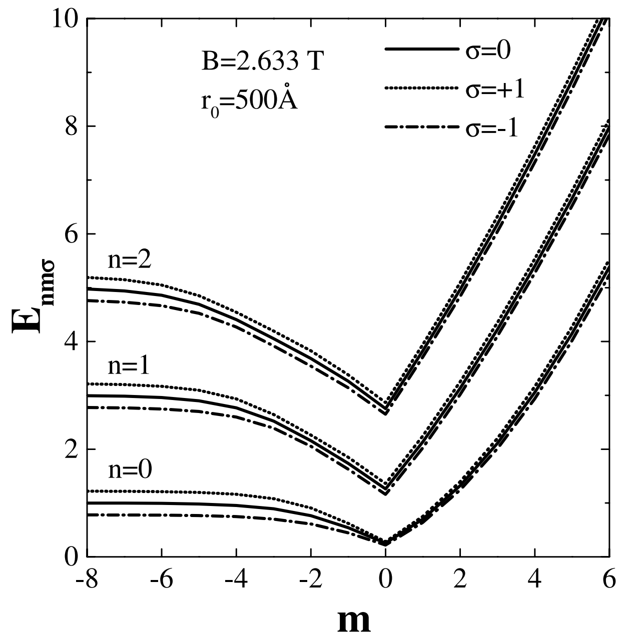

Figure 1. The dependence of the energy eigenvalues $E_{nm\sigma}$ in the magnetic quantum antidot on the angular momentum m for $r_0 = 500$ Å, $B = 2.633$ T (corresponding to $s = 5$ in reference [19]).

spin but also closely related to the angular momentum m. The larger the amplitude of the angular momentum m, the greater the degree of splitting.

Figure 2 shows the dependence of the energy levels of the magnetic quantum antidot on the angular momentum m for three different magnetic fields $B = 1.316, 2.633, 5.266$ T, while the radius of the antidot is kept the same, as $r_0 = 500$ Å. It is evident that the profile for whole energy levels resembles that exhibited in figure 1. However, the energy splittings between states with opposite spins are revealed further and the noticeable spin-dependent features can easily be seen. As the magnetic field increases, the energy levels increase drastically. Moreover, the splittings of the energy levels due to the spin effect are further enlarged with increasing magnetic field.

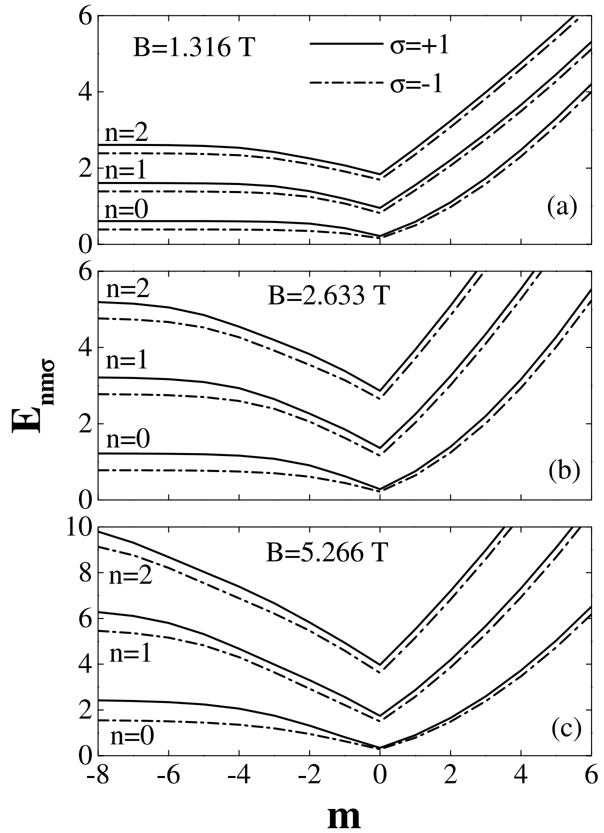

Figure 2. The dependence of the energy eigenvalues $E_{nm\sigma}$ in the magnetic quantum antidot on the angular momentum m at different magnetic fields for $r_0 = 500$ Å, with (a) $B = 1.316$ T; (b) $B = 2.633$ T; (c) $B = 5.266$ T.

Figure 3 shows the dependence of the energy levels of the magnetic quantum antidot on the angular momentum m for three values of the radius $r_0 = 250, 500, 1000$ Å, while the magnetic field is kept the same, as $B = 2.633$ T. One can not only see a noticeable spin effect but also see an obvious quantum size effect on the eigenvalues of the energy in the magnetically confined system. With increasing size of the magnetic quantum antidot, the energy levels are lowered, especially for $m > 0$, and their splittings are lessened due to the spin effect. Moreover, for smaller-size magnetic antidots, the energy is approximately linear in m for $m > 0$. From

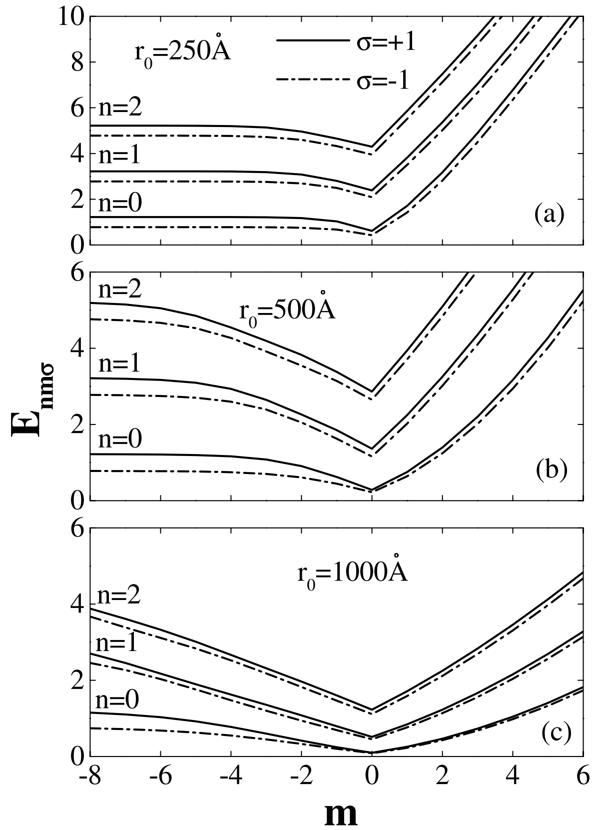

Figure 3. The dependence of the energy eigenvalues $E_{nm\sigma}$ in the magnetic quantum antidot on the angular momentum m at different radii of the magnetic antidots for $B = 2.633$ T, with (a) $r_0 = 250$ Å; (b) $r_0 = 500$ Å; (c) $r_0 = 1000$ Å.

figure 1 to figure 3, we find that the energy spectra for a magnetically confined quantum antidot not only strongly depend on the orientation of the electron spin but also strongly depend on the size of the system.

Finally, let us see how the electron spin affects the magnetoconductance spectra. We examine a two-dimensional conductor with a magnetic quantum antidot at the centre. In figure 4 we show the calculated magnetoconductance as a function of magnetic field. The Fermi energy is set to be $E_F = 2.0$ in units of $\hbar\omega_L = 1$ at $s = 5$. In this case, the magnetic fields are represented by the number of missing magnetic flux quanta s, which lie in the $\nu = 2$ quantum Hall plateau region, where ν is the Landau-level filling factor. The parameters of the structure of our model calculation are chosen to be exactly same as those in reference [19]. As it is found in reference [19], the oscillations of the magnetoconductance are not periodic, in contrast to the Aharonov–Bohm-type oscillations. Here we would like to point out that for the case which we considered in figure 4, the positions of the dips in the magnetoconductance spectra in the present work are exactly the same as those of figure 5 in reference [19]. However, the depths of the dips are quite different in the two works. The minima of most of the dips in the magnetoconductance spectra of figure 5 in reference [19] are not exactly equal to zero, while the present calculations indicate that the minima of most of the dips are equal to zero. In order to further reveal the electron spin effect and quantum size effect in the magnetic quantum

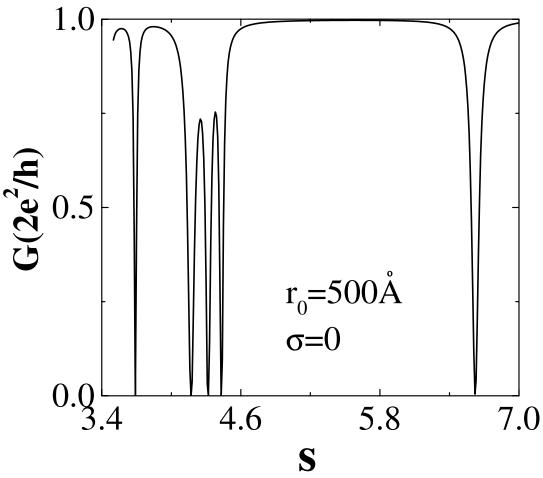

Figure 4. Magnetoconductance as a function of s for $\Gamma = 0.005$, $E_F = 2.0$, and $r_0 = 500$ Å.

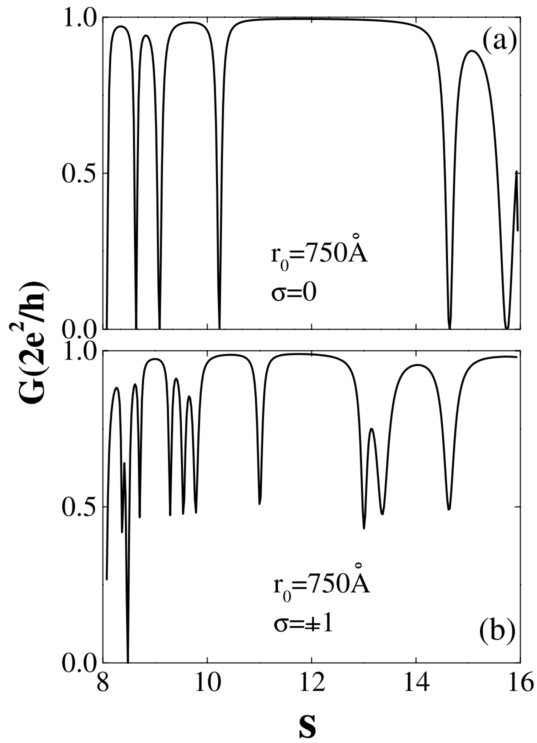

Figure 5. Magnetoconductance as a function of s for $\Gamma = 0.005$, $E_F = 2.0$, and $r_0 = 750$ Å. (a) $\sigma = 0$; (b) $\sigma = \pm 1$.

antidot, in figure 5 we give the calculated magnetoconductance as a function of magnetic field represented by the number of missing magnetic flux quanta s, which lie in the $\nu = 2$ quantum Hall plateau region. Here, $E_F = 2.0$. The radius of the magnetic quantum antidot is chosen to be $r_0 = 750$ Å. It is evident that the spin effect is not negligible; the magnetoconductance spectra are greatly changed. Compared with the case where the spin effect is not included, more dips appear and they become shallower in the magnetoconductance spectra for the case where the spin effect is included. As the size of the magnetic quantum antidot increases (see figures 4 and 5), the relative positions of the dips change greatly. The dips in the conductance are due to the resonant backscattering via the magnetic edge states [19]. In figure 6, we present the energy spectra as functions of the number of missing magnetic flux quanta s. The energy unit is assigned to have $\hbar\omega_L = 1$ at $\varphi = 5$. The different energy levels are labelled with the corresponding quantum numbers (n, m). The points of crossover between the dotted line for $E_F = 2.0$ and the energy levels give the positions of the dips in the magnetoconductance spectra for the case where the spin effect is not included. When the spin effect is taken into account, each energy curve splits into two curves, and the crossover points become double. It is noted that some of the crossover points may be located outside the magnetic region presented. Therefore, more dips appear when the spin effect is included.

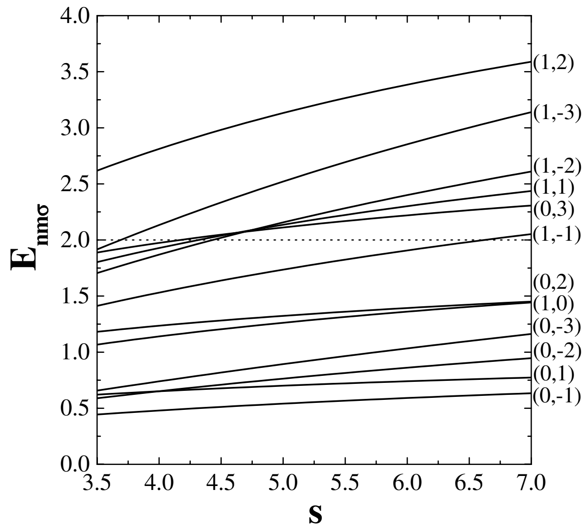

Figure 6. Energy spectra as functions of s for $\sigma = 0$. Dotted lines represent the Fermi level $E_F = 2.0$. $r_0 = 500$ Å.

4. Conclusions

We have investigated the electron spin effect and quantum size effect on the eigenenergy and the magnetoconductance in a magnetic quantum antidot. The energy levels are closely related to the angular momentum in the magnetically confined system due to the inhomogeneous magnetic field, in contrast to the case for a homogeneous magnetic field. When the spin effect is taken into account, the energy levels split further, and the splitting features are also closely related to the angular momentum. The larger the amplitude of the angular momentum, the greater the splitting of the energy levels. The magnetoconductance also shows obvious spin-dependent features. Compared with the case where the spin is not included, more and shallower dips appear in the magnetoconductance spectra due to the existence of a greater number of magnetic edge states. Moreover, the quantum size effect on the magnetic quantum antidot is noticeable, as for the usual quantum dot.

Acknowledgments

Four of us (Yong Guo, Bin Wang, Hui Hu, and Bing-Lin Gu) would like to acknowledge the partial support of this project by the National High Technology Development Programme of China (Grant No 715-010-0011) and by the Research Foundation of Tsinghua University (Grant No 98jc082).

References

[1] McCord M A and Awschalom D D 1990 *Appl. Phys. Lett.* **57** 2153
[2] Leadbeater M L, Allen S J, DeRosa J F, Harbison J P, Sands T, Ramesh R, Florez L T and Keramidas V G 1991 *J. Appl. Phys.* **69** 4689
Krishnan K M 1992 *Appl. Phys. Lett.* **61** 2365
Roy W V, Carpi E L, Von Hove M, Van Esch A, Bogaerts R, De Boeck J and Borghs G 1993 *J. Magn. Magn. Mater.* **121** 197
Yagi R and Iye Y 1993 *J. Phys. Soc. Japan* **62** 1279
[3] Geim A K 1989 *Pis. Zh. Eksp. Teor. Fiz.* **50** 359
Bending S J, von Klitzing K and Ploog K 1990 *Phys. Rev. Lett.* **65** 1060
[4] Carmona H A, Geim A K, Nogaret A, Main P C, Foster T J, Henini M, Beaumont S P and Blamire M G 1995 *Phys. Rev. Lett.* **74** 3009
[5] Ye P D, Weiss D, Gerhards R R, Seeger M, von Klitzing K, Eberl K and Nickel H 1995 *Phys. Rev. Lett.* **74** 3013
[6] Izawa S, Katsumoto S, Endo A and Iye Y 1995 *J. Phys. Soc. Japan* **64** 706
[7] Matulis M, Peeters M F and Vasilopoulos P 1994 *Phys. Rev. Lett.* **72** 1518
[8] Guo Y, Gu B L, Duan W H and Zhang Y 1997 *Phys. Rev.* B **55** 9314
[9] Guo Y, Gu B L, Li Z Q, Yu J Z and Kawazoe Y 1998 *J. Appl. Phys.* **83** 4545
[10] Guo Y, Gu B L, Li Z Q, Zhu J L and Kawazoe Y 1998 *J. Phys.: Condens. Matter* **10** 1549
[11] Guo Y, Wang H, Gu B L and Kawazoe Y 2000 *Phys. Rev.* B **61** 1728
[12] Ibrahim I S and Peeters F M 1995 *Phys. Rev.* B **52** 17 321
Krakovsky A 1996 *Phys. Rev.* B **53** 8469
[13] Yevtushenko O M and Richter K 1998 *Phys. Rev.* B **57** 14 839
[14] Geim A K, Grigorieva I V, Dubonos S V, Lok J G S, Maan J C, Filippov A E and Peeters F M 1997 *Nature* **390** 259
[15] Geim A K, Dubonos S V, Lok J G S, Grigorieva I V, Maan J C, Hansen L T and Lindelof P E 1997 *Appl. Phys. Lett.* **71** 2379
[16] Peeters F M, Matulis A and Ibrahim I S 1996 *Physica* B **227** 131
[17] Reijniers J, Peeters F M and Matulis A 1999 *Phys. Rev.* B **59** 2817
[18] Solimany L and Kramer B 1995 *Solid State Commun.* **96** 471
[19] Sim H S, Ahn K H, Chang K J, Ihm G, Kim N and Lee S J 1998 *Phys. Rev. Lett.* **80** 1501
[20] Majumdar A 1996 *Phys. Rev.* B **54** 11 911
Dobrovolsky V N, Sheka D I and Chenyachuk B V 1998 *Surf. Sci.* **397** 333
[21] Viña L 1999 *J. Phys.: Condens. Matter* **11** 5929
[22] Kikkawa J M, Smorchkova I P, Samarth N and Awschalom D D 1997 *Science* **277** 1284
[23] Monsma D J, Vlutters R and Lodder J C 1998 *Science* **281** 407
[24] Auzma N N, Khandelwal P, Barrett S E, Pfeiffer L N and West K W 1998 *Science* **281** 686
Khandelwal P, Barrett S E, Pfeiffer L N and West K W 1998 *Phys. Rev. Lett.* **81** 673
[25] Persson M, Petterson J, Sydow B V, Lindelof P E, Kristensen A and Berggren K F 1995 *Phys. Rev.* B **52** 8921
[26] Berggren K F, Ji Z L and Lundberg T 1996 *Phys. Rev.* B **54** 11 612
[27] Zeng J Y 1990 *Quantum Mechanics* (Beijing: Science) p 100